



PAPER • OPEN ACCESS

Unusual transient absorption dynamics of silver nanoparticles in solutions of carboxylated amine complexons

To cite this article: G P Shevchenko *et al* 2016 *Adv. Nat. Sci. Nanosci. Nanotechnol.* **7** 035002

View the [article online](#) for updates and enhancements.

Related content

- [Restructuring of plasmonic nanoparticle aggregates with arbitrary particle size distribution in pulsed laser fields](#)
A E Ershov, A P Gavriilyuk, S V Karpov et al.
- [Synthesis of uniform and high-density silver nanoparticles by using *Peltophorum pterocarpum* plant extract](#)
Matheswaran Balamurugan, Natesan Kandasamy, Shanmugam Saravanan et al.
- [Sensing using plasmonic nanostructures and nanoparticles](#)
Judith Langer, Sergey M Novikov and Luis M Liz-Marzán

Unusual transient absorption dynamics of silver nanoparticles in solutions of carboxylated amine complexons

G P Shevchenko¹, V A Zhuravkov¹, E V Tretyak¹, S A Tikhomirov²,
O V Buganov², A N Ponyavina², Hong Minh Pham³, Hoang Tung Do³,
Van Duong Pham³ and Dai Hung Nguyen³

¹ Research Institute for Physical Chemical Problems, Belarusian State University, 14 Leningradskaya Street, 220030 Minsk, Republic of Belarus

² B I Stepanov Institute of Physics, National Academy of Sciences of Belarus, 68 Prospekt Nezavisimosti, 220072 Minsk, Republic of Belarus

³ Institute of Physics, Vietnam Academy of Science and Technology, 18 Hoang Quoc Viet, Cau Giay, Hanoi, Vietnam

E-mail: stik@presidium.bas-net.by

Received 6 May 2016

Accepted for publication 16 May 2016

Published 5 July 2016



CrossMark

Abstract

We present the results of research on fast relaxation dynamics in the electronic excitation of silver nanoparticles synthesized in the presence of carboxylated amine complexons (NTA, Na₂EDTA, DTPA) without any reductant or polymeric stabilizer. Unusual transient absorption dynamics in these objects after femtosecond laser irradiation was found, manifesting as the appearance of an additional long-lived bleaching band. The effect may be assigned to the inhomogeneous and porous shell of silver nanoparticles synthesized by such a procedure, as the consequence of a partial fragmentation of this shell due to heating under femtosecond laser excitation of plasmonic nanoparticles and subsequent electron–phonon energy relaxation.

Keywords: silver nanoparticle sol, localized surface plasmon resonance, carboxylated amine complexons, fast relaxation dynamics, femtosecond laser pulses


Classification numbers: 2.03, 2.04, 4.02

1. Introduction

At the present time, the nanoscaled noble metals are the key objects for a new field of nano-optics—nanoplasmonics [1]. A characteristic feature of these systems is an appearance of so-called localized surface plasmon resonances (LSPR) of absorption at the optical spectra and strong enhancement of electromagnetic fields near a nanoparticle surface. Such nanoparticle-containing systems can be used in spectroscopic techniques with very high detection sensitivity—such as surface enhanced Raman scattering (SERS), surface enhanced

fluorescence (SEF)—and in the development of efficient light energy conversion systems [2–4]. The effect of surface plasmon amplification of stimulated emission of radiation near the plasmonic nanoparticle surface has also been used to create surface plasmon lasers (spasers) [5, 6]. Localized surface plasmon resonance (LSPR) is a useful and sensitive probe for the study of electronic dynamics of nanosized metal particle-based systems in pico- and femtosecond time scales [7, 8]. Such studies have a practical focus, in particular, for the construction of ultrafast optical modulators.

Generally used methods to produce metal nanoparticles [9, 10] are based on the reduction of metal ions in aqueous solutions in the presence of high-molecular compounds as stabilizers and surfactants, most of which are significantly toxic [11]. Moreover, the polymer film formed on the surface of the plasmonic nanoparticles greatly affects the LSPR

 Original content from this work may be used under the terms of the [Creative Commons Attribution 3.0 licence](https://creativecommons.org/licenses/by/3.0/). Any further distribution of this work must maintain attribution to the author(s) and the title of the work, journal citation and DOI.

spectral characteristics and weakens local field near the plasmonic nanoparticles. This reduces the efficiency of plasmonic nanostructures that would be used in highly sensitive spectroscopic techniques such as SERS and SEF and in solving problems of biosensor technique. The proposed method [12–14] of silver nanoparticle synthesis in the presence of ligands without silver ion reducing agent and polymer stabilizers is of interest in this regard.

This paper presents research results about the morphology characteristics, LSPR stationary absorption spectra and fast relaxation dynamics in the electronic excitation of silver nanoparticles synthesized in the presence of carboxylated amine complexons (NTA, Na₂EDTA, DTPA) without any reductant or polymeric stabilizer.

2. Experimental

To produce silver sols, aqueous solutions of 0.01 M AgNO₃, 0.075 M NaOH, 0.006 M NTA, 0.008 M DTPA, 0.008 M Na₂EDTA were used. The synthesis was carried out as described in [12]. A significant influence of synthesis conditions of silver sols on their optical spectra and, accordingly, their size and morphology was found. Therefore, our experiments studied the sols obtained by using different orders of component mixing. In the ‘standard’ procedure, the reaction medium was obtained by mixing the solutions of a ligand and NaOH to an operating pH value; then the reaction medium was thermostated for 20 min at 80 °C. After that the silver nitrate solution was quickly added to the hot reaction medium under vigorous stirring; the mixture obtained was maintained for 20 min at 80 °C. In the ‘nonstandard’ procedure, the reaction medium was obtained by mixing a ligand solution at a pH value within 3.2–4.6 (depending on the ligand quantity) with the silver nitrate solution; then the reaction medium was thermostated for 20 min at 80 °C. After that the NaOH solution was quickly added, under vigorous stirring, to the hot reaction medium; the mixture obtained was maintained for 20 min at 80 °C. The concentration of silver was 5.10⁻⁴ mol l⁻¹ in all the sols produced. Molar ratios of Ag⁺/L are: Ag⁺/Na₂EDTA = 1.5/1; Ag⁺/DTPA = 2/1; Ag⁺/NTA = 1/1. Value of pH was 12.0 in all cases. For comparison, a silver sol was synthesized by using sodium borohydride as an Ag⁺-ion reducer and polyvinyl alcohol as a stabilizer.

Spectral kinetic characteristics of the samples were measured using a femtosecond spectrometer [8] based on the original femtosecond pulses generator, i.e. a titanium–sapphire laser synchronously pumped by the second harmonic of a picosecond Nd:YAG laser.

Studied sol samples of approximately the same optical density in the range 0.6–0.7 were excited in 2 mm quartz cuvettes at a wavelength of 395 nm by the second harmonic of the titanium–sapphire laser. The excitation pulse duration was ~140 fs, energy ~25 μJ, spot diameter ~2 mm. Femtosecond supercontinuum emission was used as the probe pulse. Optical density variations ΔD were calculated by the formula $\Delta D(\lambda, t) = \lg(T_0/T)$, where $T = I_{\text{prob}}/I_{\text{ref}}$ and $T_0 = I_{\text{prob}}^0/I_{\text{ref}}^0$

are the energy ratio of the probe and reference pulses passing through the sample with and without excitation respectively. Δt is the time interval between excitation and probe pulses.

Samples of the silver sols were examined by optical spectroscopy (OS) and transmission electron microscopy (TEM). A dual-beam spectrophotometer Cary500 was used for registration of the absorption spectra in the wavelength range 200–800 nm. A 1 cm quartz cuvette was employed for the measurements; the dilution of the sols was four-fold. The morphology and size distribution of the sols were determined using TEM with EM-125 K.

3. Experimental results and discussion

Figure 1 shows the TEM images and size distributions for the silver sols synthesized with both the use of sodium borohydride as an Ag⁺-ion reducer and in the presence of the abovementioned complexons for the different synthesis options. It is worthwhile to note that a large-scale aggregation (of the order of 300–600 nm) observed in some TEM images does not reflect a real morphology of the studied samples but is only related to the features of sample preparation for taking TEM images.

As seen in figure 1, the particle size distribution in silver sols depends on synthesis conditions and complexon nature. The average particle size of silver sols synthesized in the presence of Na₂EDTA or DTPA varies slightly and lies in the range of 24–38 nm.

Silver sols synthesized in the presence of NTA are characterized by a narrow particle size distribution and smaller particle sizes as compared with those of silver sols synthesized in the presence of Na₂EDTA or DTPA. Thus, in the first case (NTA, figure 1(b)), the proportion of particles with sizes less than 10 nm is 30%, while in the other case (Na₂EDTA or DTPA)—less than 10%. Then, in the case of NTA, nanoparticles have square or stretched shape as compared to more spherical shape in the cases of Na₂EDTA or DTPA.

The silver sol obtained with borohydride reduction has the smallest silver particles (mean size 4 nm) and is most mono-dispersed. The same trend of mixing order dependence for all sols was observed. In the case of nonstandard synthesis procedure, the obtained sols are characterized by smaller particle sizes (1.2–1.5 times) and a narrower particle size distribution as compared with the sols obtained by standard synthesis procedure.

As seen in the insets of figure 2, the particles observed are not homogeneous but have dense cores and a porous shell consisting of finer nanoparticles of sizes in the range of 5–10 nm. The existence of fine nanoparticles near the large inhomogeneous silver nanoparticles was also observed. The silver sol obtained with borohydride is made of particles of very small size (<10 nm), substantially non-aggregated, unlike the sols with complexons. The observed difference in structure of the silver particles synthesized in the presence of complexons or borohydride is due to the different mechanisms of their formation.

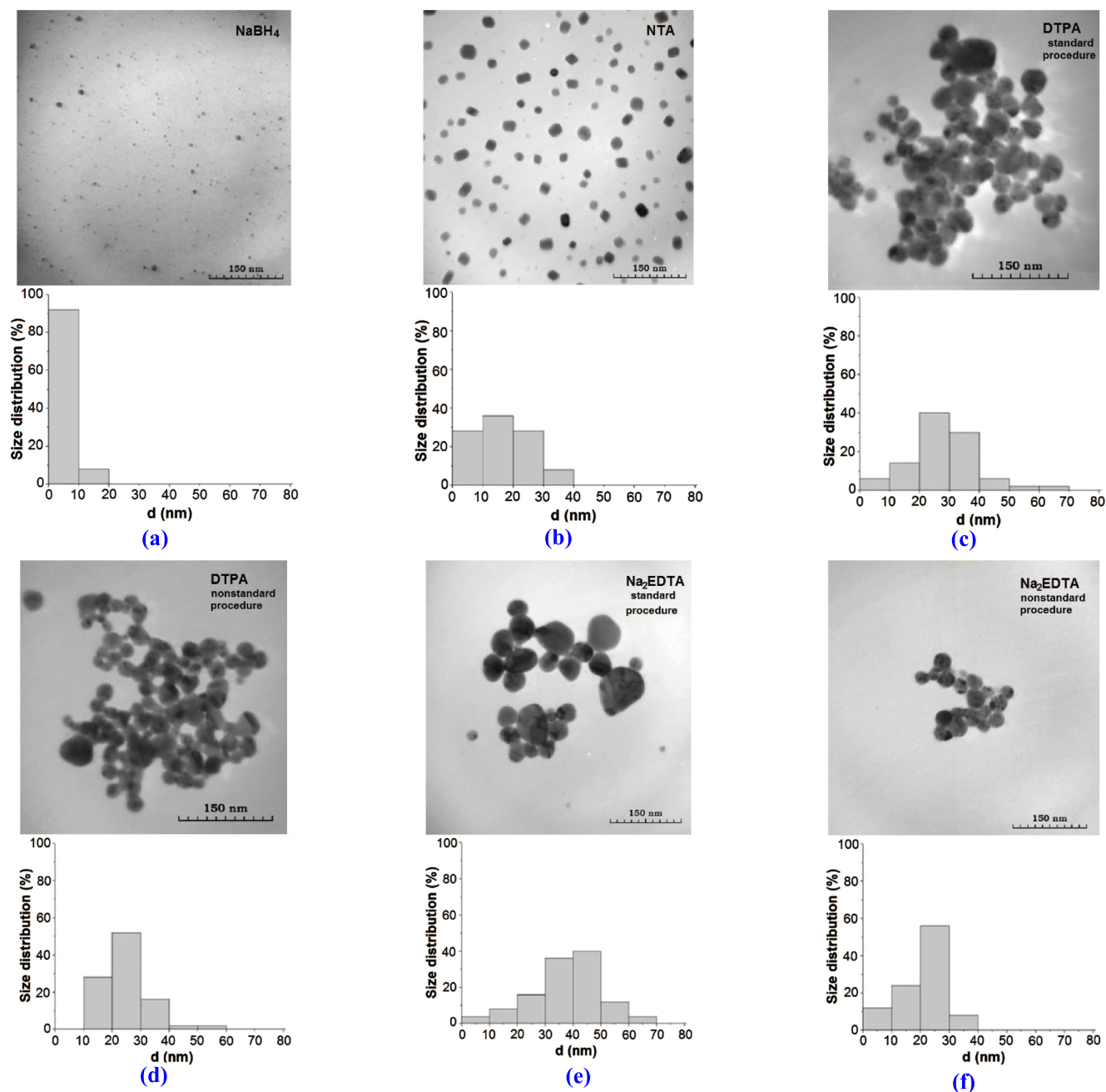
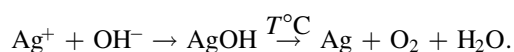


Figure 1. TEM images and size distributions of the silver particles in sols obtained with different synthesis option and procedure: NaBH_4 (a), NTA (b), DTPA (c), (d) and Na_2EDTA (e), (f). [b, d, f—nonstandard and c, e—standard procedure].

As we have established [12, 13], the formation of silver nanoparticles in the presence of complexons occurs in alkaline medium and at elevated temperature through the formation of AgOH and its further thermal decomposition in accordance with the reactions:



Under such conditions the concentration of silver ions, formed as a result of the dissociation of the AgL complex, in the reaction medium is largely determined by the stability constant of a complex in solution ($K_{\text{stab.AgL}}$) of AgL . The

formation of AgOH becomes possible at such a concentration of silver ions when the ion product (IP) of AgOH exceeds the solubility product (SP): $\text{IP}_{\text{AgOH}} > K_{\text{SP}(\text{AgOH})} = 1.6 \times 10^{-8}$ [12]. Calculations show that for the complexons used this requirement is achieved, depending on the value of $K_{\text{stab.AgL}}$, at a certain ratio of Ag^+/L : with an increase in the $K_{\text{stab.AgL}}$ value this ratio should be greater than 1. Taking into account this mechanism of silver nanoparticle formation in the presence of complexons (without reducing agent), the growth of particles, presumably, proceeds according to the mechanism of colloidal aggregation of primary particles [15]. Dissociating AgL complexes are suppliers of silver ions in solution and after dissociation a chelator acts as a stabilizer of metal silver

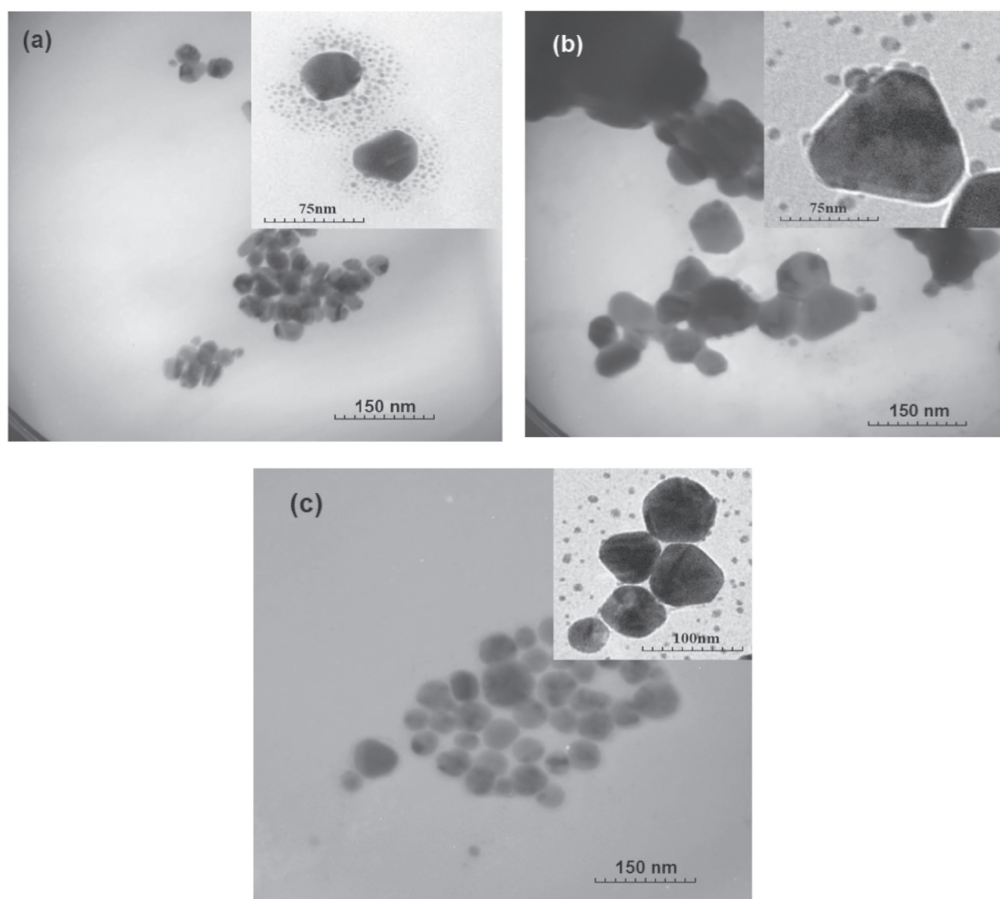


Figure 2. TEM pictures of the silver particles in sols obtained in presence of different ligands: NTA (a), DTPA (b), Na₂EDTA (c); insets correspond to the increase of resolution.

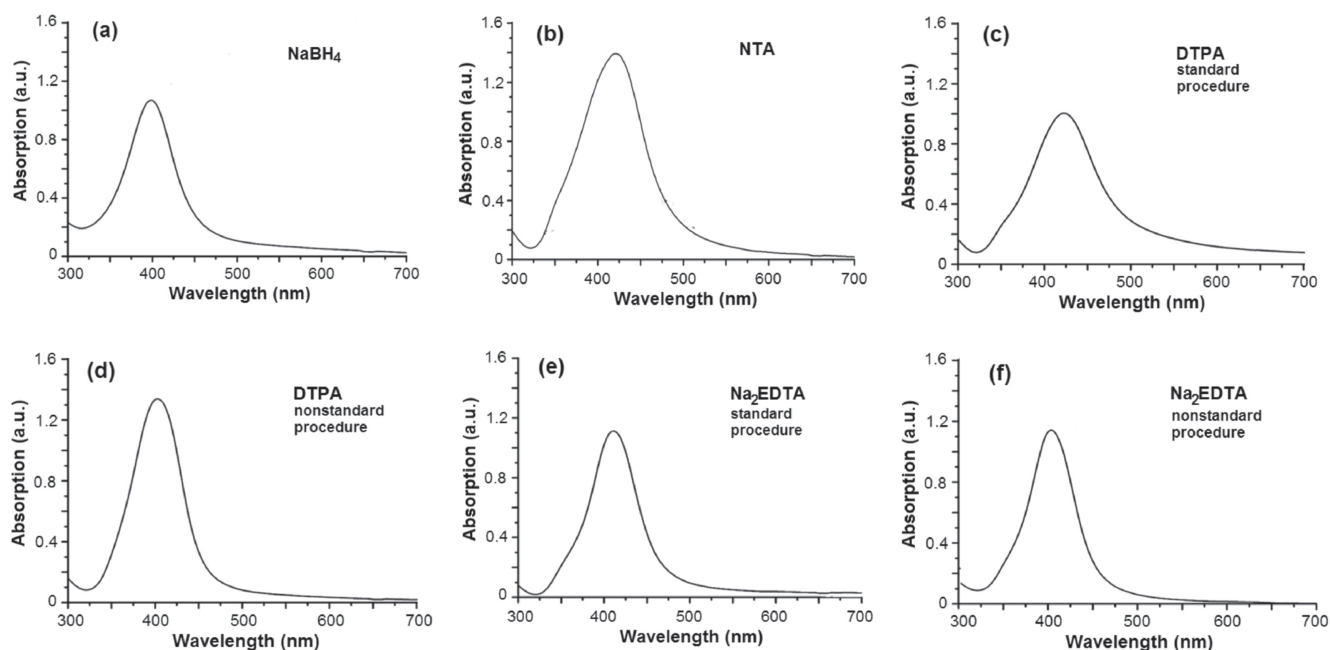


Figure 3. Stationary spectra of the silver sols obtained with different synthesis option and procedure: in the presence of NaBH₄ (a), NTA (b), DTPA (c), (d), Na₂EDTA (e), (f). [b, d, f—nonstandard; c, e—standard synthesis procedure].

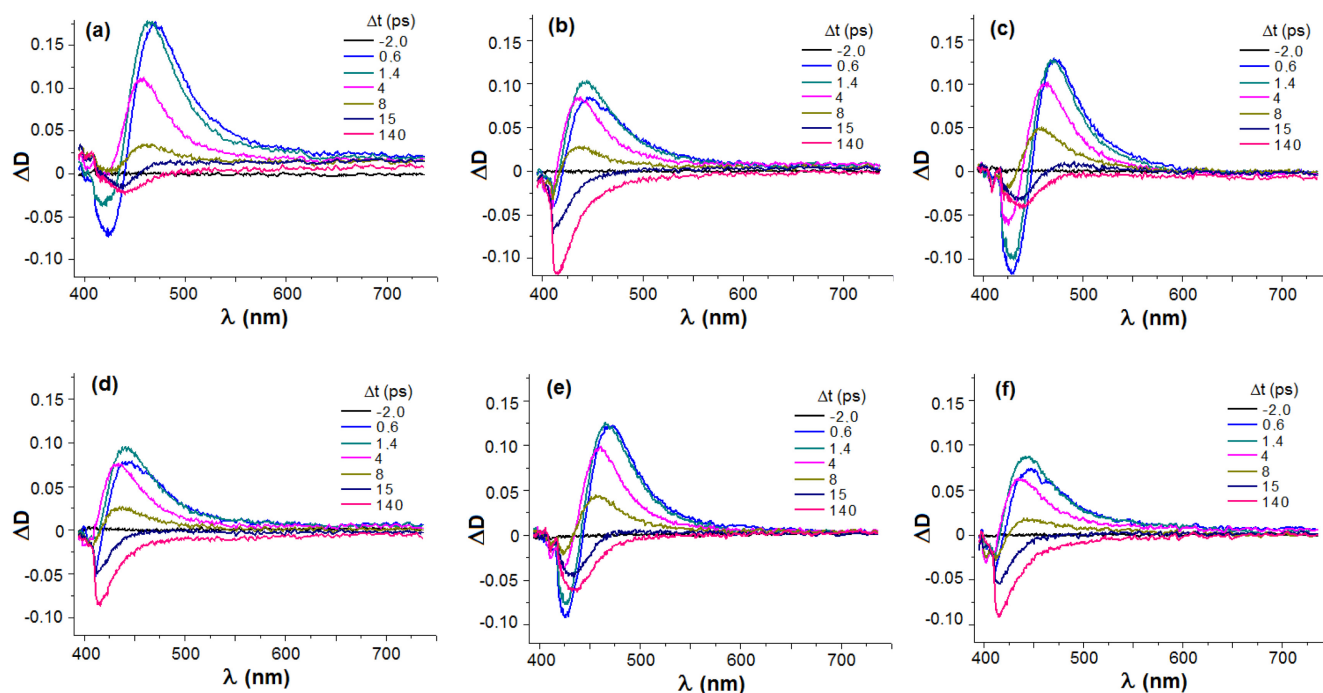


Figure 4. Transient absorption spectra of the silver sols obtained with different synthesis options: in the presence of NaBH_4 (a), NTA (b), DTPA (c), (d) and Na_2EDTA (e), (f). [b, d, f—nonstandard; c, e—standard synthesis procedure].

nanoparticles. In accordance with the mechanism mentioned above, non-uniform silver nanoparticles with a denser core and porous shell are formed. In contrast, in the presence of borohydride the growth of silver particles occurs due to the autocatalytic reduction of silver ions on the primary particles, therefore they are solid.

Figure 3 shows the steady-state absorption spectra for the silver sols obtained with the different synthesis procedures. As one can see, the spectral position of the localized surface plasmon resonance (LSPR) maxima varies from 400 nm to 421 nm, the LSPR half-width from 65 nm to 89 nm, and the optical density at the LSPR maxima from 1.0 to 1.7. The LSPR characteristics depend on both the mean size of silver nanoparticles and the half-width of the size distribution function. In particular, the analysis from figures 1–3 shows that the size decrease of silver nanoparticles synthesized by the nonstandard procedure is accompanied by a short-wavelength shift of the LSPR maximum as compared with that synthesized by the standard procedure. It could be mentioned that the sol obtained with NTA, despite a narrow particle size distribution and a large proportion of minor particles (figure 1), has the highest value of spectral LSPR half-width strip—equal to 89 nm (figure 3(b)).

Figure 4 shows the differential transient absorption spectra of silver nanoparticles in studied sols obtained with different delay time (Δt) between the excitation and probe pulses in the LSPR spectral range. As usual there are a rapidly relaxing bleaching (negative ΔD) within the LSPR band maximum (in the experiment only the long-wavelength part of the bleaching band is recorded due to the limited spectral sensitivity of the detector in the region ≤ 420 nm) and induced absorption in the longer wavelength region. This indicates the

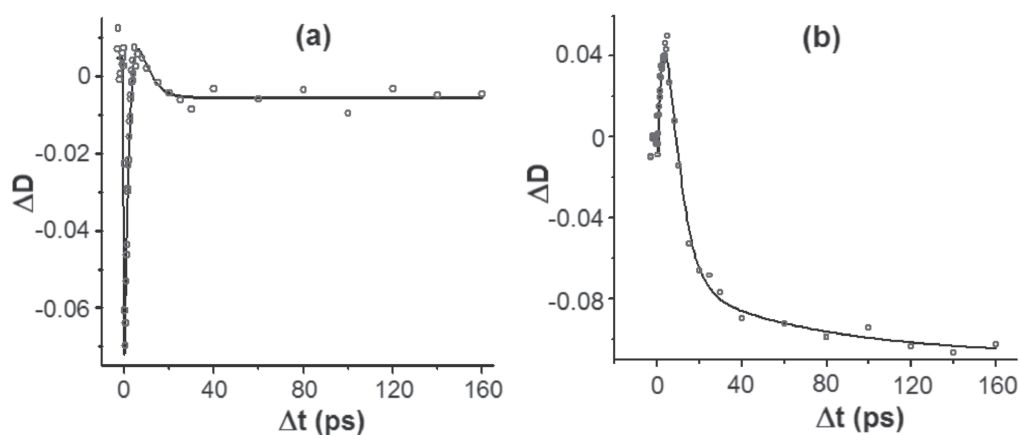
transformation of the absorption spectra as a result of the changes of plasmonic nanoparticle electron temperature when they are excited by femtosecond pulses, namely, their broadening and decrease in intensity. The process of cooling of electrons inside the particle is due to electron–phonon interactions, occurs within a few picoseconds and generates a fast (picoseconds) component of the induced optical density kinetics.

Of particular interest is the fact that in all studied sols at the delays in the range of 15–140 ps, a new bleaching band is formed. This band is 10–35 nm shifted to the longer wavelength range as compared to the stationary spectra (except of the sol with NTA, a nonstandard option). It can be interpreted as the result of the LSPR band narrowing or as displacement of the LSPR band to shorter wavelengths in this time range. Full recovery of the system occurs in the nanosecond time range and at the time of the experiment this looks like a disappearance of the additional bleaching band. Along with the common features in the transient absorption spectra of all studied sols, there are some differences depending on the complexon nature and the synthesis options. Thus, for non-standard sols with smaller particles there is a more significant transient spectra intensity change in the area of the second bleaching band. For the sol obtained with borohydride, the additional bleaching band manifests itself very poorly.

Table 1 given below lists the main experimental parameters of the investigated sols depending on the synthesis options and the complexon nature. The parameters are: mean size of silver nanoparticles (d_{aver}), position of the LSPR maximum and the LSPR half-width at stationary absorption spectra ($\lambda^{\text{s}}_{\text{max}}$, $\Delta\lambda^{\text{s}}$), as well as position and intensity of the

Table 1. Characteristics of silver sols obtained with various synthesis procedures.

Sols	d_{aver} (nm)	λ_{max}^s (nm)	$\Delta\lambda^s$ (nm)	$\lambda_{\text{max}}^{\text{ns}}Z$ (nm)	$-\Delta D_{\text{max}}^{\text{ns}}$
Borohydrid	4	400	65	435	0.022
NTA (nonstandard)	19	421	89	<413	0.118
DTPA (standard)	29	411	68	437	0.041
DTPA (nonstandard)	24	404	63	<415	0.084
Na ₂ EDTA (standard)	38	420	78	437	0.061
Na ₂ EDTA (nonstandard)	22	403	66	<414	0.090

**Figure 5.** Transient absorption kinetics at 420 nm wavelength: (a) sol with NaBH₄ and (b) sol with NTA.

second bleaching band in differential transient absorption spectrum of the silver sols ($\lambda_{\text{max}}^{\text{ns}}$, $\Delta D_{\text{max}}^{\text{ns}}$).

It may be noted that for varied complexons the difference in intensity of the additional bleaching band is observed. As mentioned above, almost all investigated samples have maximum of an additional bleaching band ($\lambda_{\text{max}}^{\text{ns}}$) located at longer wavelengths relative to the LSPR maximum in the corresponding stationary spectrum (λ_{max}^s). Reducing the silver particle size or the half-width of size distribution function in the case of the nonstandard procedures, the manifestation of the additional bleaching band is accompanied by a short-wavelength shift of the transient absorption spectrum as compared with the case of standard procedures. The situation observed when using chelator NTA must be noted. In this case, the maximum of the additional bleaching band (413 nm) realizes in the short-wave region relative to the LSPR maximum in the corresponding stationary absorption spectrum (421 nm).

Figure 5 shows the transient absorption kinetics at 420 nm wavelength for silver nanoparticles obtained with NaBH₄ and without it in the presence of the complexons. As mentioned, the cooling of electrons inside a particle due to electron–phonon interactions occurs within the picosecond time range and generates a fast (several picoseconds) component in the bleaching relaxation kinetics. This component is present in the kinetics of all studied sols. Origin of the ‘longer’ growing component corresponding to the long-lived long-wave bleaching band (figure 5(b)), is unusual and requires special consideration. We believe that this may be due to the internal inhomogeneity and pore structure of silver nanoparticles formed by the mechanism of colloidal

aggregation in the presence of a chelating carboxyalkyl amine series. Reversible changes in mean size and internal structure of the primary non-homogeneous porous nanoparticles under the influence of laser radiation can induce corresponding reversible changes in the spectral position and half-width of LSPR band. This finds its expression in the emergence of long-lived long-wavelength additional bleaching band at the differential transient spectra.

It can be assumed that under the influence of a short laser pulse excitation the size of the large ‘loose’ particles (about 60 nm) decreases as a consequence of the fragmentation of the porous shell into small (about 5 nm) isolated particles. Indeed, as mentioned, in our experiment silver nanoparticles are produced in the presence of complexons.

They are not solid, but are the aggregates of smaller particles. Energy excitation stored in the particles may dissipate as heat to the environment (water with complexon and NaOH), which can lead to its heating. Such heating takes place also within a porous shell, consisting of small particles. Intensification of the Brownian motion of the molecules in the pores of the primary silver nanoparticles promotes the moving apart of smaller silver nanoparticles that form a loose shell, and partial destruction of this shell—the primary porous nanoparticle starts to break up. An additional circumstance contributing to significant heating of the porous shell can be a huge gain of local fields, which is caused by the dense packing of small silver nanoparticles in the shell [14].

The increase of the total fraction of small particles shifts the LSPR maximum to shorter wavelengths. Hereupon the differential transient spectra show additional bleaching in the spectral range of the stationary LSPR band. The exact spectral

position of the additional bleaching band is determined by the type of complexons and synthesis conditions. Furthermore, it should be noted that the LSPR characteristics of silver nanoparticles with a 'loose' shell of smaller particles depend on the degree of the shell porosity, which defines the value of its effective permittivity ϵ_{eff} [16]. 'Swelling' of the shell due to heating of the medium during the relaxation of the electronic excitation energy of nanoparticles caused by the influence of a femtosecond laser pulse leads to a change of ϵ_{eff} and a long-wavelength shift of the Fröhlich frequency [16]. This effect can compete with a short-wavelength displacement of the LSPR caused by the fragmentation of large particles with a porous shell.

A number of papers (see, for example, [17–22]) have been devoted to a nonreversible size/shape change of noble metal (silver, gold, copper, nickel) nanoparticles, which were affected by laser radiation at a wavelength corresponding to their LSPR spectral range. These changes are associated with the particles' temperature change due to an irradiation, which depends on the properties of the laser excitation (energy density, pulse duration, the time of exposure, etc), and on the parameters of the irradiated system (stabilizer type, reducing agent nature, amount and shape of particles). Calculations show [23] that irreversible changes of the silver 10–100 nm particle shape will occur at an energy density in the range 5–10 mJ cm⁻² when the temperature of the particles can exceed the melting point of the material. At an energy density greater than 60 mJ cm⁻² the particle size changes due to their evaporation and particle fragmentation must be observed. The largest particles are fragmented primarily as they have a larger volume and cross section, thereby they absorb the largest fraction of the laser radiation [20]. Such a destruction of large particles into smaller ones leads to a shift of absorption maxima to shorter wavelengths. The authors of [20] note that the carrier storage on a surface of nanoparticles of 40–60 nm due to their ionization under laser radiation may also lead to their fragmentation and small particle formation.

All the aforementioned cases lead to irreversible changes in particle size and shape. Small particle formation resulting from large particle destruction due to both overheating and ionization is accompanied by the shift of the LSPR maxima to shorter wavelengths. In the differential transient absorption spectra, this phenomenon presents as a nonreversible bleaching at the spectral range of the LSPR maxima. In our experiments, the recorded changes are completely reversible and the system restores its initial state within a few nanoseconds. In our opinion, this can be a sequence and a competition of two processes as follows: (i) the process of porous nanoparticle fragmentation under the influence of laser pulses of small energy and duration and (ii) the self-assembly process of a reconstruction of porous conglomerates from small nanoparticles.

Previously marked differences in the transient absorption spectra between the NTA silver sols and the DTPA and Na₂EDTA sols are, apparently, connected to chelator properties [24]. The NTA has a low complexing ability and denticity (K_{st} for silver complexes with NTA–5.4, EDTA–7.3, DTPA–8.7 [25]), as well as smaller molecule sizes as

compared with the other complexons used. All these NTA features affect the morphology of silver particles formed—for example, along with rounded particles arise nanorods up to 100 nm with a thickness of 20–25 nm [26]. The stability and the optical spectra of the sols are affected as well. Likewise, these NTA features, naturally, should affect the behavior of the transient absorption spectra under femtosecond laser excitation in the LSPR spectral range. This subject requires further specific research.

4. Conclusion

Unusual transient absorption dynamics of silver nanoparticles synthesized in the presence of the carboxylated amine complexons was found. An additional long-time bleaching band was registered at transient absorption spectra of these sols. It was established that the spectral position and intensity of the induced bleaching band depends on the type of complexon used at the nanoparticle synthesis. The effect may be connected with the inhomogeneous and porous shell of silver nanoparticles synthesized by such a procedure and as the consequence of a partial fragmentation of this shell due to heating of the medium after femtosecond laser excitation of plasmonic nanoparticles and stored energy relaxation. Reported differences of the NTA silver sols transient absorption spectra, as compared with that of the DTPA and Na₂EDTA sols, is apparently related to the structural features of the NTA molecule, its low denticity and complexing ability.

Acknowledgments

The financial support from Vietnam Academy of Science and Technology to authors through Project VAST 01.05/14-15 and VAST.HTQT.Belarus.02/13-14 is greatly acknowledged.

References

- [1] Kik P G and Brongersma M L 2007 *Surface Plasmon Nanophotonics* (Netherlands: Springer)
- [2] Johansson P 2005 *Phys. Rev. B* **72** 035427
- [3] Zhang J and Lakowicz J R 2005 *J. Phys. Chem. B* **109** 8701
- [4] Heard S M, Grieser F, Barraclough C G and Sanders J V 1983 *J. Coll. Interface Sci.* **93** 545
- [5] Bergman D J and Stockman M J 2003 *Phys. Rev. Lett.* **90** 027402
- [6] Stockman M I 2008 *Nat. Photon.* **2** 327
- [7] Link S and El-Sayed M A 2003 *Annu. Rev. Phys. Chem.* **54** 331
- [8] Buganov O V, Zamkovets A D, Ponyavina A N, Tikhomirov S A and Baran L V 2011 *J. Appl. Spectros* **78** 686
- [9] Loginov A V, Gorbunova V V and Boytsova T V 1997 *Russ. J. Gen. Chem.* **67** 189
- [10] Sigimoto T 1987 *Adv. Colloid Interface Sci.* **28** 65
- [11] Meng C, Ying L, Han J T, Zhang J Y, Li Z Y and Qian D L 2006 *J. Phys. Chem. B* **110** 11224

- [12] Shevchenko G P, Zhuravkov V A, Tretyak E V, Shautsova V I and Gaiduk P I 2014 *Physicochem. Eng. Aspects* **446** 65
- [13] Shevchenko G P and Tretyak E V 2008 Nanostructure materials *Proc. First Int. Conf. (NANO-2008) (Minsk, Belarus, 22–25 April 2008)* 149
- [14] Shautsova V I, Zhuravkov V A, Korolik O V, Novikau A G, Shevchenko G P and Gaiduk P I 2014 *Plasmonics* **9** 993
- [15] Yakutik I M, Shevchenko G P and Rakhmanov S K 2004 *Colloid. Surf. A: Physicochem. Eng. Aspects* **242** 175
- [16] Shevchenko G P, Ponyavina A N, Kachan S M, Afanas'eva Z M and Gurin V S 2003 *J. Appl. Spec.* **70** 405
- [17] Unal A, Stalmashonak A, Graener H and Seifert G 2009 *Phys. Rev. B* **80** 115415
- [18] Seifert G, Stalmashonak A, Hofmeister H, Haug J and Dubiel M 2009 *Nanoscale Res. Lett.* **4** 1380
- [19] Stalmashonak A, Seifert G and Graener H 2007 *Opt. Lett.* **32** 3215
- [20] Kamat P V, Flumiant M and Hartland G V 1998 *J. Phys. Chem. B* **102** 3123
- [21] Tsuji T, Watanabe N and Tsuji M 2003 *Appl. Surf. Sci.* **211** 189
- [22] Stietz F 2001 *Appl. Phys. A* **72** 381
- [23] Tarasenko N, Butsen A, Shevchenko G and Yakutik I 2005 *Sol. Stat. Phenomena* **106** 27
- [24] Dyatlova N M, Ya T V and Popov K I 1988 *Complexones and Metal Complexonates* (Moscow: Khimiya) 112
- [25] Martell A E and Smith R M 1982 *Critical Stability Constants* (New York: Springer)
- [26] Shevchenko G P, Zhuravkov V A, Tretyak E V, Shautsova V I and Gaiduk V I 2014 *Colloid. Surf. A: Physicochem. Eng. Aspects* **446** 65